Supplement: Exotic photonic molecules via Lennard-Jones-like potentials

Przemyslaw Bienias,[1,2] Michael J. Gullans,[1,2,3] Marcin Kalinowski,[1,4] Alexander N. Craddock,[1]
Dalia P. Ornelas-Huerta,[1] Steven L. Rolston,[1] J.V. Porto,[1] and Alexey V. Gorshkov[1,2]

[1] *Joint Quantum Institute, NIST/University of Maryland, College Park, Maryland 20742 USA*
[2] *Joint Center for Quantum Information and Computer Science, NIST/University of Maryland, College Park, Maryland 20742 USA*
[3] *Department of Physics, Princeton University, Princeton, New Jersey 08544 USA*
[4] *Faculty of Physics, University of Warsaw, Pasteura 5, 02-093 Warsaw, Poland*

(Dated: July 31, 2020)

Here, we present the derivation of effective interactions between polaritons propagating through Rydberg media close to the Förster resonance (sec. I), derivation of the characteristic energy and length scales in the two-body problem (sec. II), derivation of the single-channel description used to give intuition behind three-body forces (sec. III), and self-consistent solution of the four body problem (sec. IV).

I. TWO PHOTONS PROPAGATING THROUGH RYDBERG MEDIA CLOSE TO THE FÖRSTER RESONANCE

Here, we give more details related to the effective interactions between Rydberg states described by Eq. (**??**) in the main text. Our model system is a one-dimensional gas of atoms whose electronic levels are given in Fig. 1(a) in the main text. Following Ref. [S1–S4], we introduce operators $\hat{I}^\dagger(z)$ and $\hat{S}^\dagger(z)$ which generate the atomic excitations into the $|I\rangle$ and $|S\rangle$ states, respectively, at position z. In addition, comparing to Ref. [S1–S5] we include a more complex atomic level structure of the source and the gate excitations by defining $\hat{P}_1^\dagger(z)$ and $\hat{P}_2^\dagger(z)$ which create excitations into $|P_1\rangle$ and $|P_2\rangle$ states, respectively. All the operators $\hat{O}(z) \in \{\hat{\mathcal{E}}(z), \hat{I}(z), \hat{S}(z), \hat{P}_1(z), \hat{P}_2(z)$ are bosonic and satisfy the equal time commutation relation, $[\hat{O}(z), \hat{O}^\dagger(z')] = \delta(z-z')$.

The microscopic Hamiltonian describing the propagation consists of three parts: $\hat{H} = \hat{H}_{\rm p} + \hat{H}_{\rm ap} + \hat{H}_{\rm int}$. For the sake of simplicity we show the derivation for the 1D massive photons, which straightforwardly applies to the free-space photons within the center of mass frame, and generalizes to a 2D cavity. The first term describes the photon evolution in the medium and is defined as

$$\hat{H}_{\rm p} = -\frac{1}{2m_{\rm ph}} \int dz \hat{\mathcal{E}}^\dagger(z) \partial_z^2 \hat{\mathcal{E}}(z), \tag{S1}$$

with the mass defined by the cavity geometry. The atom-photon coupling is described by

$$\hat{H}_{\rm ap} = \int dz \Big[g\hat{\mathcal{E}}(z)\hat{I}^\dagger(z) + \Omega \hat{S}^\dagger(z)\hat{I}(z) + g\hat{I}(z)\hat{\mathcal{E}}^\dagger(z) + \Omega \hat{I}^\dagger(z)\hat{S}(z) + \Delta \hat{I}^\dagger(z)\hat{I}(z) \Big], \tag{S2}$$

where g is the collective coupling of the photons to the matter, and for the sake of brevity we drop the decay rates γ_S, γ_{P_1} and γ_{P_2}. The interaction between Rydberg levels is described by

$$\hat{H}_{\rm int} = \frac{1}{2} \int dz' \int dz \begin{pmatrix} \hat{S}\hat{S} \\ \hat{P}_1\hat{P}_2 \\ \hat{P}_2\hat{P}_1 \end{pmatrix}^\dagger \begin{pmatrix} V_{SS} & V_d & V_d \\ V_d^* & V_{PP}+\Delta_d & V_{PP,\rm off} \\ V_d^* & V_{PP,\rm off} & V_{PP}+\Delta_d \end{pmatrix} \begin{pmatrix} \hat{S}\hat{S} \\ \hat{P}_1\hat{P}_2 \\ \hat{P}_2\hat{P}_1 \end{pmatrix}, \tag{S3}$$

where the notation was explained in the main text. The Schroedinger equation has the form

$$i\hbar\partial_t |\psi(t)\rangle = \hat{H} |\psi(t)\rangle, \tag{S4}$$

with the two-excitation wavefunction having the form [S2, S5]

$$\begin{aligned} |\psi(t)\rangle = \int {\rm d}z \int {\rm d}z' \Big[& \frac{1}{2}\mathcal{E}\mathcal{E}(z,z',t)\hat{\mathcal{E}}^\dagger(z)\hat{\mathcal{E}}^\dagger(z') + \frac{1}{2}PP(z,z',t)\hat{P}^\dagger(z)\hat{P}^\dagger(z') + \frac{1}{2}SS(z,z',t)\hat{S}^\dagger(z)\hat{S}^\dagger(z') \\ & + \mathcal{E}P(z,z',t)\hat{\mathcal{E}}^\dagger(z)\hat{P}^\dagger(z') + \mathcal{E}S(z,z',t)\hat{\mathcal{E}}^\dagger(z)\hat{S}^\dagger(z') + PS(z,z',t)\hat{P}^\dagger(z)\hat{S}^\dagger(z') + P_1P_2(z,z',t)\hat{P}_1^\dagger(z)\hat{P}_2^\dagger(z') \Big] |0\rangle . \end{aligned} \tag{S5}$$

The Schroedinger equation [S2] in the frequency space reduces to

$$\omega\mathcal{EE}(z,z') = -\frac{1}{2m_{\rm ph}}\left(\partial_z^2+\partial_{z'}^2\right)\mathcal{EE}(z,z') + g(\mathcal{E}I(z,z')+\mathcal{E}I(z',z)), \tag{S6}$$

$$\omega\mathcal{E}I(z,z') = \left(-\frac{1}{2m_{\rm ph}}\partial_z^2+\Delta\right)\mathcal{E}I(z,z') + gII(z,z') + \Omega\mathcal{E}S(z,z'), \tag{S7}$$

$$\omega\mathcal{E}S(z,z') = \left(-\frac{1}{2m_{\rm ph}}\partial_z^2+\Delta\right)\mathcal{E}S(z,z') + gIS(z,z') + \Omega\mathcal{E}I(z,z'), \tag{S8}$$

$$\omega II(z,z') = 2\Delta II(z,z') + g(\mathcal{E}I(z,z')+\mathcal{E}I(z',z)) + \Omega(IS(z,z')+IS(z',z)), \tag{S9}$$

$$\omega IS(z,z') = \Delta IS(z,z') + g\mathcal{E}S(z,z') + \Omega SS(z,z'), \tag{S10}$$

$$\omega SS(z,z') = \Omega(IS(z,z')+IS(z',z)) + V_{SS}(z-z')SS(z,z') + V_d(z-z')\left(P_1P_2(z,z')+P_1P_2(z',z)\right), \tag{S11}$$

$$\omega P_1P_2(z,z') = V_d^*(z-z')SS(z,z') + V_{PP}(z-z')P_1P_2(z,z') + \Delta_d P_1P_2(z,z') + V_{PP,\rm off}(z-z')P_1P_2(z',z), \tag{S12}$$

where only the two last equations differ from the conventional one [S1–S4].

Next, we eliminate the P_1P_2 component

$$P_1P_2(z,z') = \frac{V_d^*(z-z')}{\omega - V_{PP}(z-z') - \Delta_d - V_{PP,\rm off}(z-z')}SS(z,z'), \tag{S13}$$

which is not coupled by the laser field directly to photons. This leads to

$$\omega SS(z,z') = \left(V_{SS}(z-z') - \frac{2V_d(z-z')^2}{\Delta_d + V_{PP}(z-z') + V_{PP,\rm off}(z-z') - \omega}\right)SS(z,z') + \Omega(IS(z,z')+IS(z',z)). \tag{S14}$$

Note that $S(z,z') = S(z',z)$. We see from Eq. (S14) that the effective interaction between Rydberg states takes the form shown in Eq. (3) in the main text.

II. THE CHARACTERISTIC ENERGY AND LENGTHS SCALES IN THE TWO BODY PROBLEM

Let us next comment in more detail on the form of the $V_f(r)$ given by Eq. (**??**) in the main text. Since $|V_f| \ll \omega_c$, the depth of V_e is nearly equal to the depth of V_f in the considered regime, and is given by $V_{\rm min} = -(\sqrt{2}C_3 - \sqrt{C_{SS}\left(\Delta_d-\omega\right)})^2/C_{PP}$; note that we consider states for which $C_{PP}, C_{SS}>0$. The minimum of the potential occurs at the relative distance given by $r^6 = C_{PP}\sqrt{C_{SS}}/\left(\sqrt{2}C_3\sqrt{\Delta_d-\omega} - \sqrt{C_{SS}}(\Delta_d-\omega)\right)$, which leads to a characteristic length scale $b = \left(\left(\sqrt{2}+1\right)C_{PP}C_{SS}/C_3^2\right)^{1/6}$, by taking $\Delta_d = \nu_c/2$ with $\nu_c = 2C_3^2/C_{SS}$. The potential's local minimum exists for $C_{SS}\left(\omega-\Delta_d\right)+2C_3^2 > 0$. For $\omega = 0$ and $\epsilon = \Delta_d/\nu_c < 1$ we have $V_{\rm min} = -2C_3^2\left(\sqrt{\epsilon}-1\right)^2/C_{PP}$. Therefore, we define $V_c = 2C_3^2/C_{PP}$, which together with ν_c is used as a characteristic energy scale in our results.

III. COMPARISON OF SINGLE-CHANNEL PP VS DOUBLE-CHANNEL P_1P_2 PHYSICS

We illustrate the relation between the effective PP channel description (i.e., Eq. (**??**) in the main text) and the two channels P_1P_2 and P_2P_1 description for the three-body problem. For the sake of simplicity we neglect weaker off-diagonal vdW interactions $V_{PP,\rm off}$.

We consider the Hamiltonian in the following basis: $|SSS\rangle$, $|SP_1P_2\rangle$, $|SP_2P_1\rangle$, $|P_1SP_2\rangle$,$|P_1P_2S\rangle$, $|P_2SP_1\rangle$, and $|P_2P_1S\rangle$. The off-diagonal part of the Hamiltonian:

$$\begin{pmatrix}
0 & \frac{e^{2i\phi_{2,3}}C_d}{r_{2,3}^3} & \frac{e^{2i\phi_{2,3}}C_d}{r_{2,3}^3} & \frac{e^{2i\phi_{1,3}}C_d}{r_{1,3}^3} & \frac{e^{2i\phi_{1,2}}C_d}{r_{1,2}^3} & \frac{e^{2i\phi_{1,3}}C_d}{r_{1,3}^3} & \frac{e^{2i\phi_{1,2}}C_d}{r_{1,2}^3} \\
\frac{e^{-2i\phi_{2,3}}C_d}{r_{2,3}^3} & 0 & 0 & \frac{C_{d,1}}{r_{1,2}^3} & 0 & 0 & \frac{C_{d,2}}{r_{1,3}^3} \\
\frac{e^{-2i\phi_{2,3}}C_d}{r_{2,3}^3} & 0 & 0 & 0 & \frac{C_{d,1}}{r_{1,3}^3} & \frac{C_{d,2}}{r_{1,2}^3} & 0 \\
\frac{e^{-2i\phi_{1,3}}C_d}{r_{1,3}^3} & \frac{C_{d,1}}{r_{1,2}^3} & 0 & 0 & \frac{C_{d,2}}{r_{2,3}^3} & 0 & 0 \\
\frac{e^{-2i\phi_{1,2}}C_d}{r_{1,2}^3} & 0 & \frac{C_{d,1}}{r_{1,3}^3} & \frac{C_{d,2}}{r_{2,3}^3} & 0 & 0 & 0 \\
\frac{e^{-2i\phi_{1,3}}C_d}{r_{1,3}^3} & 0 & \frac{C_{d,2}}{r_{1,2}^3} & 0 & 0 & 0 & \frac{C_{d,1}}{r_{2,3}^3} \\
\frac{e^{-2i\phi_{1,2}}C_d}{r_{1,2}^3} & \frac{C_{d,2}}{r_{1,3}^3} & 0 & 0 & 0 & \frac{C_{d,1}}{r_{2,3}^3} & 0
\end{pmatrix}, \tag{S15}$$

whereas the diagonal one

$$\begin{pmatrix} \frac{C_{\rm SS}}{r_{1,2}^6}+\frac{C_{\rm SS}}{r_{1,3}^6}+\frac{C_{\rm SS}}{r_{2,3}^6} \\ \frac{C_{P_1P_2}}{r_{2,3}^6}+\Delta_d+\frac{C_{\rm SP_1}}{r_{1,2}^6}+\frac{C_{\rm SP_2}}{r_{1,3}^6} \\ \frac{C_{P_1P_2}}{r_{2,3}^6}+\Delta_d+\frac{C_{\rm SP_2}}{r_{1,2}^6}+\frac{C_{\rm SP_1}}{r_{1,3}^6} \\ \frac{C_{P_1P_2}}{r_{1,3}^6}+\Delta_d+\frac{C_{\rm SP_1}}{r_{1,2}^6}+\frac{C_{\rm SP_2}}{r_{2,3}^6} \\ \frac{C_{P_1P_2}}{r_{1,2}^6}+\Delta_d+\frac{C_{\rm SP_1}}{r_{1,3}^6}+\frac{C_{\rm SP_2}}{r_{2,3}^6} \\ \frac{C_{P_1P_2}}{r_{1,3}^6}+\Delta_d+\frac{C_{\rm SP_2}}{r_{1,2}^6}+\frac{C_{\rm SP_1}}{r_{2,3}^6} \\ \frac{C_{P_1P_2}}{r_{1,2}^6}+\Delta_d+\frac{C_{\rm SP_2}}{r_{1,3}^6}+\frac{C_{\rm SP_1}}{r_{2,3}^6} \end{pmatrix}, \tag{S16}$$

where C_d denotes dipolar interactions between SS and P_1P_2, $C_{d,1}$ between SP_1 and P_1S, and $C_{d,2}$ between SP_2 and P_2S. Terms without index $_d$ denote vdW interactions.

In order to present the following argument, it is enough to consider only the Hamiltonian elements between five states (out of seven) which we do for the clarity of presentation: We rotate the interaction Hamiltonian into the symmetric and asymmetric basis $|SSS\rangle$, $\frac{1}{\sqrt{2}}(|SP_1P_2\rangle \pm |SP_2P_1\rangle)$, and $\frac{1}{\sqrt{2}}(|P_1SP_2\rangle \pm |P_2SP_1\rangle)$. The off-diagonal terms are:

$$\begin{pmatrix} 0 & \frac{\sqrt{2}e^{2i\phi_{2,3}}C_d}{r_{2,3}^3} & 0 & \frac{\sqrt{2}e^{2i\phi_{1,3}}C_d}{r_{1,3}^3} & 0 \\ \frac{\sqrt{2}e^{-2i\phi_{2,3}}C_d}{r_{2,3}^3} & 0 & \frac{\left(C_{\rm SP_2}-C_{\rm SP_1}\right)\left(r_{1,2}^6-r_{1,3}^6\right)}{2r_{1,2}^6r_{1,3}^6} & \frac{C_{d,1}+C_{d,2}}{2r_{1,2}^3} & \frac{C_{d,1}-C_{d,2}}{2r_{1,2}^3} \\ 0 & \frac{\left(C_{\rm SP_2}-C_{\rm SP_1}\right)\left(r_{1,2}^6-r_{1,3}^6\right)}{2r_{1,2}^6r_{1,3}^6} & 0 & \frac{C_{d,1}-C_{d,2}}{2r_{1,2}^3} & \frac{C_{d,1}+C_{d,2}}{2r_{1,2}^3} \\ \frac{\sqrt{2}e^{-2i\phi_{1,3}}C_d}{r_{1,3}^3} & \frac{C_{d,1}+C_{d,2}}{2r_{1,2}^3} & \frac{C_{d,1}-C_{d,2}}{2r_{1,2}^3} & 0 & \frac{\left(C_{\rm SP_2}-C_{\rm SP_1}\right)\left(r_{1,2}^6-r_{2,3}^6\right)}{2r_{1,2}^6r_{2,3}^6} \\ 0 & \frac{C_{d,1}-C_{d,2}}{2r_{1,2}^3} & \frac{C_{d,1}+C_{d,2}}{2r_{1,2}^3} & \frac{\left(C_{\rm SP_2}-C_{\rm SP_1}\right)\left(r_{1,2}^6-r_{2,3}^6\right)}{2r_{1,2}^6r_{2,3}^6} & 0 \end{pmatrix}, \tag{S17}$$

whereas the diagonal one:

$$\begin{pmatrix} C_{\rm SS}\left(\frac{1}{r_{1,3}^6}+\frac{1}{r_{2,3}^6}+\frac{1}{r_{1,2}^6}\right) \\ \frac{C_{P_1P_2}}{r_{2,3}^6}+\Delta_d+\frac{1}{2}C_{\rm SP_1}\left(\frac{1}{r_{1,3}^6}+\frac{1}{r_{1,2}^6}\right)+\frac{1}{2}C_{\rm SP_2}\left(\frac{1}{r_{1,3}^6}+\frac{1}{r_{1,2}^6}\right) \\ \frac{C_{P_1P_2}}{r_{2,3}^6}+\Delta_d+\frac{1}{2}C_{\rm SP_1}\left(\frac{1}{r_{1,3}^6}+\frac{1}{r_{1,2}^6}\right)+\frac{1}{2}C_{\rm SP_2}\left(\frac{1}{r_{1,3}^6}+\frac{1}{r_{1,2}^6}\right) \\ \frac{C_{P_1P_2}}{r_{1,3}^6}+\Delta_d+\frac{1}{2}C_{\rm SP_1}\left(\frac{1}{r_{2,3}^6}+\frac{1}{r_{1,2}^6}\right)+\frac{1}{2}C_{\rm SP_2}\left(\frac{1}{r_{2,3}^6}+\frac{1}{r_{1,2}^6}\right) \\ \frac{C_{P_1P_2}}{r_{1,3}^6}+\Delta_d+\frac{1}{2}C_{\rm SP_1}\left(\frac{1}{r_{2,3}^6}+\frac{1}{r_{1,2}^6}\right)+\frac{1}{2}C_{\rm SP_2}\left(\frac{1}{r_{2,3}^6}+\frac{1}{r_{1,2}^6}\right) \end{pmatrix}. \tag{S18}$$

From the off-diagonal terms we see the $\sqrt{2}$ enhancement of the coupling from SS to the symmetric-superposition channel denoted by the PP in the main text. Coefficients C_{PP}, C_{SP} in the main text correspond to the averages of corresponding two-channel quantities.

We see that for the generic geometry with $r_{ij} \neq r_{jk}$, decoupling from asymmetric channels requires $C_{SP_1} \approx C_{SP_2}$ and $C_{d,1} \approx C_{d,2}$. In our proposal we use $n_1 = n$ and $n_2 = n-1$ with $n = 120 \gg 1$ for which $C_{SP_1}/C_{SP_2} \approx 0.98$ $C_{d,1}/C_{d_2} \approx 0.92$. This enables us to use the effective single-channel picture to give an intuition behind the multi-body forces. Note that all the numerical results presented in the main text are performed without the single-channel approximation. Finally, the single-channel picture is valid only for two- and three-body problem.

IV. FOUR-BODY PROBLEM

The four-body problem features additional exotic phenomena due to the strong four-body interactions. For ^{87}Rb, the ground state is a configuration consisting of two far-separated dimers [S6], see Fig. S1(a). However for ^{133}Cs, which has $C_{SP}/C_{PP} \approx 0.6$ (compared with $C_{SP}/C_{PP} \approx 1.4$ for ^{87}Rb) and therefore weaker multi-body forces, the ground state configuration depends on Δ_d, Fig. S1(b): the ground state is a linear configuration for $\Delta_d/\nu_c \geq 0.3$ and two far-separated dimers for $\Delta_d/\nu_c \leq 0.3$ [S7].

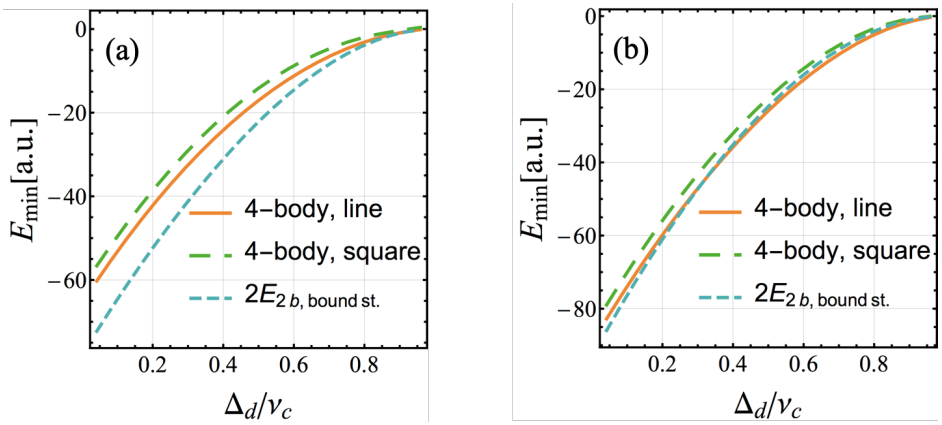

FIG. S1. Self-consistent solution of Eq. (6) in the main text describing polaritons in the large-mass limit. (a-b) Lowest energy as a function of Δ_d for line, regular-polygon, and dimer configurations for four bodies. Results are shown in (a) for ^{87}Rb and in (b) for ^{133}Cs; all of them are for n_1, n_2, n as in Fig. 2 in the main text.

[S1] A. V. Gorshkov, J. Otterbach, M. Fleischhauer, T. Pohl and M. D. Lukin, *Photon-photon interactions via Rydberg blockade*, Phys. Rev. Lett., **107**, 133602 (2011).

[S2] T. Peyronel, O. Firstenberg, Q. Y. Liang, S. Hofferberth, A. V. Gorshkov, T. Pohl, M. D. Lukin and V. Vuletić, *Quantum nonlinear optics with single photons enabled by strongly interacting atoms*, Nature, **488**, 57–60 (2012).

[S3] P. Bienias, S. Choi, O. Firstenberg, M. F. Maghrebi, M. Gullans, M. D. Lukin, A. V. Gorshkov and H. P. Büchler, *Scattering resonances and bound states for strongly interacting Rydberg polaritons*, Phys. Rev. A, **90**, 053804 (2014).

[S4] H. Gorniaczyk, C. Tresp, P. Bienias, A. Paris-Mandoki, W. Li, I. Mirgorodskiy, H. P. Büchler, I. Lesanovsky and S. Hofferberth, *Enhancement of Rydberg-mediated single-photon nonlinearities by electrically tuned Förster resonances*, Nat. Commun., **7**, 12480 (2016).

[S5] P. Bienias, *Few-body quantum physics with strongly interacting Rydberg polaritons*, Eur. Phys. J. Spec. Top., **225**, 2957–2976 (2016).

[S6] Which we checked is independent of n, i.e., n mostly rescales the length and energy scales.

[S7] Note that for the linear configuration, the optimal distance between the edge and middle particles is smaller than the distance between the two particles in the middle, however, these distances differ by less than 1%, and in the plots we simply use the average of these distances.